Applied Catalysis B: Environmental 84 (2008) 372–378

Contents lists available at ScienceDirect

Applied Catalysis B: Environmental

journal homepage: www.elsevier.com/locate/apcatb

Electrochemically assisted photocatalytic degradation of methyl orange using anodized titanium dioxide nanotubes

Yon S. Sohn, York R. Smith, Manoranjan Misra, Vaidyanathan (Ravi) Subramanian *

Department of Chemical & Metallurgical Engineering, Mail Stop 388, University of Nevada, Reno, 1664 North Virginia Street, Reno, NV 89431, USA

ARTICLE INFO

Article history:
Received 8 February 2008
Received in revised form 11 April 2008
Accepted 14 April 2008
Available online 25 April 2008

Keywords:
Titanium dioxide nanotubes
Anodization
Photocatalysis
Methyl orange
Electrocatalysis

ABSTRACT

The TiO_2 nanotubes have demonstrated potential in the photoelectrocatalytic degradation of methyl orange dye (MO). TiO_2 nanotubes were prepared using anodization of titanium foils in phosphoric acid (PA) and ethylene glycol (EG) by mechanical stirring and ultrasonic method. The TiO_2 nanotubes prepared in EG under ultrasound followed by annealing in nitrogen atmosphere showed higher activity towards dye degradation as compared to the stirring method. Dye degradation shows improved activity under an external bias compared to degradation performed in the absence of an external bias. An increase in the external bias from +0.0 to +0.1 V versus calomel electrode (SCE) is sufficient to improve the degradation rates of MO from 22% to 57% within the first 10 min. At +0.1 V, a complete degradation of 40 μM MO is observed within 30 min. The addition of oxidants such as oxygen and hydrogen peroxide demonstrate improvement in the MO degradation.

1. Introduction

The presence of dye pollutants in the wastewater streams from the textile industry are of an enormous environmental concern. It is estimated that nearly 15% of the dye is lost during dyeing processes and is released into wastewater streams [1]. These dyeing effluents can have toxic effects on the ecosystem, especially on microorganisms, and its long degradation time in the environment is a cause for concern. A variety of physical, chemical, and biological methods are presently utilized in wastewater treatment systems. Though biological treatment is a proven technology and is cost-effective, it has been reported that the majority of dyes are only adsorbed on the sludge and are not degraded [2]. Physical methods, such as ion-exchange [3], adsorption [4], air stripping [5], etc., simply transfer the pollutants to another phase rather than destroying them.

Titanium dioxide has emerged as the leading candidate to provide complete destruction of organic pollutants via heterogeneous photocatalysis that result in total mineralization of many organic pollutants [6,7]. Several studies have been reported of using TiO_2 slurry in photocatalytic degradation of different dyes [8–10]. Though this process offers actual annihilation of the dye molecules at a very high efficiency, the post-treatment recovery of TiO_2 can be costly [11]. Thus several researchers have investigated the possibility of immobilizing TiO_2 on a substrate as a film to counter this problem [12,13]. For example, Boldrin and coworkers have demonstrated the use of sol–gel TiO_2 film on a titanium metal support [14–17]. However, there is a risk of a significant reduction of active surface area when the TiO_2 particles are cast as films. This causes the degradation time to be prolonged [18].

Recently, the synthesis of TiO_2 in the form of hollow nanotubes (NTs) over a titanium substrate has been demonstrated [19]. These nanotubes are typically produced by anodic oxidation of the titanium foil in various electrolytes [20,21]. They have demonstrated interesting photoelectrochemical activity that mainly includes water splitting [22]. A few articles on the photocatalytic degradation of pollutants have also been reported [23–25]. Different methods of producing nanotubular array of titanium dioxide that yields high photocurrent has been reported [21,22].

There are several reasons for evaluating the photocatalytic properties of TiO_2 nanotubes for dye degradation. Compared to TiO_2 nanoparticles, there are fewer interfacial grain boundaries in TiO_2 nanotubes. This has been reported to improve the redox catalytic properties at the TiO_2 surface [26]. The presence of less grain boundaries also assists in promoting charge (electron-hole) transport. Improved charge transport is known to favor photocatalytic degradation of pollutants [23]. Finally, the dimensions of the nanotubes are such that space charge layer (and related electronic properties such as band gap) in the nanotubes promote electron-hole pair separation [27]. This can also improve photocatalytic dye degradation.

* Corresponding author. Tel.: +1 775 784 4686; fax: +1 775 327 5059.
E-mail address: ravisv@unr.edu (V. (Ravi) Subramanian).

0926-3373/$ – see front matter © 2008 Published by Elsevier B.V.
doi:10.1016/j.apcatb.2008.04.021

In this paper, we have examined the photocatalytic degradation of a model dye, methyl orange (MO), over TiO_2 nanotubular anode. Methyl orange, which belongs to the azo dyes family, and is known to be carcinogenic and mutagenic, has been studied by Boldrin and coworkers [14]. We have prepared the TiO_2 nanotubes in different electrolytes by adapting an earlier reported procedure [28]. The work reported in Ref. [28] has been focused on the preparation methods of the TiO_2 nanotubes and the formation mechanism during anodization. The work reported herein compares different methods for TiO_2 nanotube synthesis and identifies the most promising method specifically from an application (i.e. photocatalytic degradation) point of view. Further, the application of external bias, effects of different oxidants on the photocatalytic degradation of dye, and an insight into the effects of additives on degradation mechanism is also presented here.

2. Experimental

2.1. Chemicals

Phosphoric acid (H_3PO_4, Fisher, 85% in water), sodium fluoride (NaF, Fischer, 99.5%), ammonium fluoride (NH_4F, Fischer, 100%), ethylene glycol ($C_2H_4(OH)_2$, Fischer), deionized water (Millipore Q®), acetone (Aldrich, 99.5%, diluted to 50%), methyl orange (Sigma), and hydrogen peroxide (H_2O_2, Aldrich, 35 wt.% in water) were used as received without further treatment. The titanium foil thickness was 0.2 mm (ESPI Metals, 99.9% purity).

2.2. Preparation of TiO_2 nanotube array

Rectangular strips (1 cm × 4 cm) of titanium foils were cut out, and were washed in acetone under ultrasonication for 5 min. Nanotubular TiO_2 arrays were formed by anodization of the titanium foils in 400 mL of electrolytic solution using 20 V_{DC} bias (Agilent E3649A DC Power Source) for 60 min. A two-electrode configuration was used for anodization against a flag shaped platinum cathode (thickness: 1 mm, area: 3.75 cm^2). The distance between the two electrodes was kept at 4.5 cm in all experiments. Only 3.5 cm of the Ti foil length was submerged in the anodization medium.

Two different anodization media – aqueous and non-aqueous – were used in these experiments to compare its effect on photodegradation reaction. The aqueous medium consisted of phosphoric acid (PA) solution (0.5 M H_3PO_4 and 0.14 M NaF). The non-aqueous medium was ethylene glycol (EG) solution (0.5 wt.% NH_4F and 10 wt.% distilled water). For both types, two different agitation mechanisms were utilized—magnetic stirring (S) and ultrasonication (U). The stirring speed was maintained at 100 rpm (Corning Stirring Hot Plate PC-420D), and the ultrasonication was carried out at 42 kHz (Branson 3510 Ultrasonicator). The four different types of samples will be referred to as PAS, PAU, EGS, and EGU here forth.

2.3. Annealing of samples

All samples were heat treated by annealing under nitrogen atmosphere at 500 °C in a tube furnace (Thermo Scientific, Lindberg Blue M BF51866C). The furnace was ramped up at a rate of 1 °C/min, and was maintained at 500 °C for 2 h. It has been reported that TiO_2 NTs prepared using EG as the anodization medium exhibits higher photoactivity for water electrolysis reaction when annealed in hydrogen atmosphere [28]. To examine the effect of annealing condition on the photocatalytic degradation process, EGU samples have been prepared in both nitrogen and hydrogen atmosphere (EGUN and EGUH, respectively, here forth).

2.4. Characterization

The scanning electron micrograph of EGUN samples was obtained using Hitachi S-4700 FE-SEM. An energy dispersion spectroscopy (EDS) analysis identifying the composition of nanotubes is also reported. The glancing-angle X-ray diffraction pattern was obtained using Philips-12045 B/3 diffractometer. The Cu Kα irradiation source was utilized at 40 kV.

2.5. Photocatalytic degradation of methyl orange

A 40 μM solution of MO was prepared in distilled water. This concentration was chosen for its UV–vis spectrum exhibiting absorbance near but below 1.0. A custom-made three-arm cell (one arm each for a working, counter and reference electrodes) was used for all photocatalytic degradation experiments. The cell holds approximately 7 mL of solution at a level where the TiO_2 electrode was submerged just below the anodization line (∼3 cm). A UV–vis light source was used to illuminate the TiO_2 photoanode (Newport 66902, Oriel Research). The far-UV radiation was filtered out using 0.5 M copper sulfate solution. The anode was kept at a 5 cm distance from the light source. The luminescence intensity was measured to be ∼90 mW/cm^2 at the photocell surface.

A potentiostat (Autolab PGSTAT 302) was used to apply an external bias during the degradation experiments. The effect of decreasing applied bias voltage was tested at +0.6, 0.5, 0.4, 0.3, 0.2, 0.1, and 0 V and under no bias conditions with respect to saturated calomel electrode (SCE). All voltages reported are versus SCE unless otherwise noted. A UV–vis absorption spectrum was obtained at 0, 10, 20, 30, 40, 50, and 60 min during the degradation experiments (Shimadzu UV2501 PC). Approximately 1 mL of the MO dye solution was taken out to obtain the spectrum and returned to the cell once the measurement was finished. The percent degradation was measured by the change in peak absorbance (at 464 nm) with respect to the absorbance at 0 min.

2.6. Effect of presence of oxidants

To investigate the effect of presence of oxidizing species, 0.5 mL of hydrogen peroxide (7.1 vol.%, 2.64 wt.%) was added to 6.5 mL of 40 μM MO solution. The experiments were performed with an external bias of +0.0 V versus SCE and also at no bias conditions under illumination. All other conditions were kept constant. The effect of oxygen saturation on photodegradation rate was studied by saturating 7 mL of 40 μM MO dye solution for 10 min prior to UV–vis illumination.

3. Results

3.1. Comparison of various anodization and annealing conditions on MO degradation

Fig. 1 shows the changes in the absorption spectra of an aqueous MO solution during the photodegradation process over the TiO_2 nanotubes. The spectra were taken at 10 min intervals of time following UV–vis illumination. The data in the figure shows the photocatalytic degradation of MO over PAS TiO_2 sample at +0.6 V in ambient condition. The absorbance spectra shown in the figure are representative of the trend noticed with other TiO_2 samples as well. The spectrum at $t = 0$ is the absorbance exhibited by the dye after equilibration in the dark with TiO_2 prior to photo-illumination. At $t = 60$ min of photo-illumination, a 54% decrease in the peak absorbance is observed. The decrease in the absorbance of MO with time was different in the presence of PAU, PAS, and EGS samples.

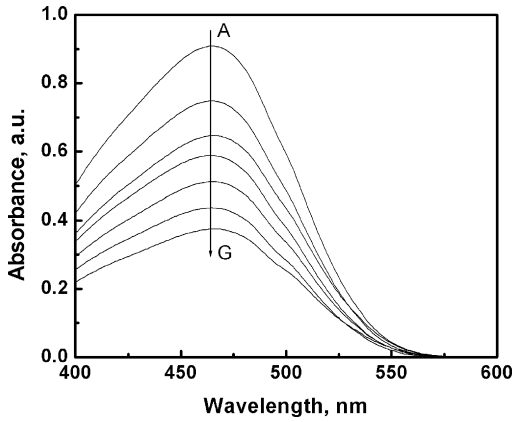

Fig. 1. Absorption spectra obtained at 10 min interval under UV–vis illumination from 0 to 60 min. The phosphoric acid stirred (PAS) sample type was used at +0.6 V versus SCE.

From Fig. 1, a steady and smooth decrease in the absorbance is noted across the wavelength range of study. Sometimes, the dye degradation can result in products that are detected as alternate peaks or shoulders in absorbance spectroscopy [29]. Fig. 1 suggests that TiO_2 nanotubes degrade the dye via a pathway that does not show such detectable products. In related studies of MO degradation over TiO_2 particles, a temporary appearance of a peak in the region associated with the aromatic compounds is observed in the near-UV region [30]. However, these peaks are reported to disappear as degradation process continues indicating a complete mineralization of the MO molecule.

For estimating the extent of degradation, the percent degradation data was calculated using Beer–Lamberts relationship between MO dye concentration and peak absorbance at 464 nm. To confirm the role that UV–vis illumination plays in the degradation process, experiments were carried out with and without illumination. Fig. 2 displays that without the UV–vis illumination, the change in the MO concentration is insignificant regardless of the magnitude of bias voltage applied (+0.0 and +0.6 V compared in Curves (A) and (B), respectively). Curve (B) shows that negligible amount of degradation (2%) occurs due to ambient lighting in the laboratory at a bias of +0.6 V. A notable 85% degradation is observed at t = 60 min when the surface of the PAU TiO_2 sample is illuminated with UV–vis light at +0.6 V (Curve (D)). This clearly indicates that the TiO_2 NTs are photocatalytically active only in the presence of direct illumination, and that electrochemical oxidation alone using TiO_2 nanotubes (without the UV–vis illumination) in the range of applied potential studied here within is insufficient to cause any significant change in the dye concentration. Blank runs with Ti foils demonstrated no change in dye absorbance in both electrochemical and photoelectrochemical processes at +0.6 V indicating that Ti foils do not demonstrate degradation. In the figure, it can also be noted that the EGS sample shows close to 100% degradation (Curve (E)).

At t = 60 min, magnetically stirred samples show 25% lower degradation compared to agitated samples prepared under ultrasonication (Curves (C) and (D), respectively) in the phosphoric acid medium. This holds true in the case of TiO_2 NTs prepared in EG to a slightly lesser degree (approximately 10% increase). However, all types of ultrasonically treated samples show near-complete degradation of the dye within 60 min of UV/vis illumination (Fig. 2 Curve (D)), Fig. 3 Curves (B) and (C)).

In comparing the NTs prepared in the two types of anodization electrolyte, superior photodegradation efficiency is observed with NTs prepared in the EG medium. A difference of 10% to 15% in the initial rate (0 to 20 min) is observed between PAU and EGUN samples. The effect of the different annealing conditions on the degradation of MO at an external bias voltage of +0.6 V was also monitored. The choice of this bias voltage was made arbitrarily based on information gathered from literature [31,32]. The effect of varying bias voltage is discussed in later sections. In Fig. 3, the difference between EGUN and EGUH is negligible and assumed to be within experimental error. Therefore, for all subsequent experiments EGUN was chosen as the sample type for further analysis.

3.2. SEM-EDS characterization of TiO_2 nanotubular catalyst

Since the TiO_2 NTs prepared in EG medium were noted to be the most active for photodegradation, surface characterization using SEM-EDS and XRD was performed on only these samples. In Fig. 4, a cursory look at the topography in the scanning electron micrographs of the TiO_2 NTs anodized in EG medium indicates that the NTs are stacked in a closely packed array adjacent and parallel to one another. An analysis of the cross-section of the anodized TiO_2 nanotubes indicates that the average length is 750 and 1000 nm for EGS and EGUN samples, respectively (a representative cross-section is shown). The inner diameter was 50 and 75 nm while the thickness was 15 and 5 nm for EGS and

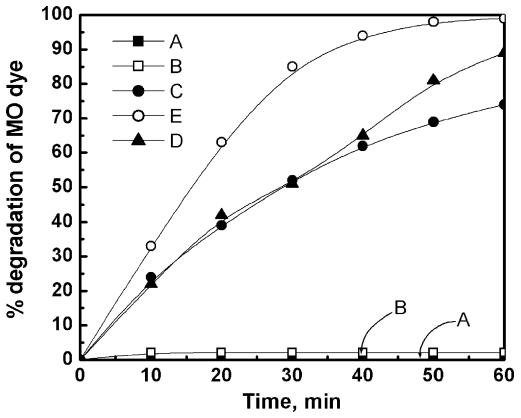

Fig. 2. Effect of applied bias on phosphoric acid stirred (PAS) samples without illumination at (A) +0.0 V and (B) +0.6 V. Effect of different samples types under UV–vis illumination at +0.6 V with (C) PAS; (D) phosphoric acid ultrasonicated (PAU); and (E) ethylene glycol stirred (EGS).

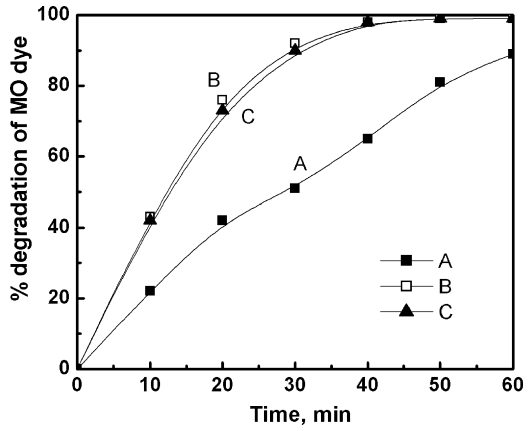

Fig. 3. Comparison of degradation over TiO_2 nanotubes prepared in ethylene glycol under different conditions: (A) ethylene glycol stirred (EGS); (B) ethylene glycol ultrasonicated and N_2 annealed (EGUN); (C) ethylene glycol ultrasonicated and H_2 annealed (EGUH). All experiments were carried out at +0.6 V under UV/vis illumination.

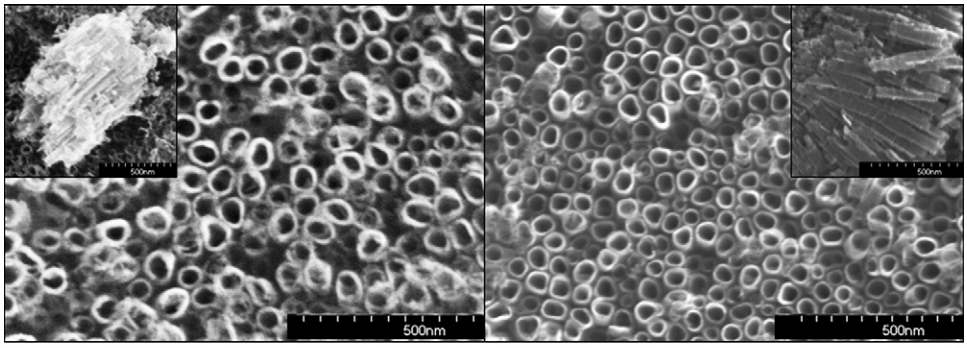

	Ti (at. %)	O (at. %)
EGS	65.24	34.76
EGUN	65.49	34.51
EGUH	65.99	34.01

Fig. 4. Scanning electron micrographs of TiO_2 nanotubes prepared in different conditions. Left: ethylene glycol stirred (EGS); right: ethylene glycol ultrasonicated and N_2 annealed (EGUN). The insets of the figure show the length of the TiO_2 nanotubes (all scale bars 500 nm). The composition of the nanotubes estimated using EDS is shown below.

EGUN samples, respectively. There was negligible difference in the physical parameters between the NTs annealed in nitrogen and hydrogen atmosphere. The energy dispersive spectra (EDS) reveal the composition of the NTs. There was no noticeable difference between EGUN and EGUH samples. Both samples showed (shown as an inset in Fig. 4) titanium and oxygen with trace amounts of vanadium (found in the Ti metal foil).

3.3. XRD analysis of TiO_2 nanotubular catalyst

The crystalline phase of the TiO_2 nanotubes was determined by glancing angle X-ray diffraction. Fig. 5 shows the XRD of the EGUN and EGUH samples ((A) and (B), respectively). The (*h k l*) values corresponding to the crystalline phases identified in each sample is also shown in the figure. The peaks were indexed against standard card from the PDF-4 database (JADE 6.0, Materials Data, Inc.). Similar observations were reported by Zlamal and coworkers [23]. Every major peak in the diffraction patterns can be accounted for between the anatase form of the oxide (PDF# 21-1272, labeled "A") and the base titanium metal (PDF# 44-1294, labeled "Ti"). It can be observed that the peaks corresponding to anatase phase, especially that of $2\theta = 38^\circ$, have higher intensity in the EGUN sample.

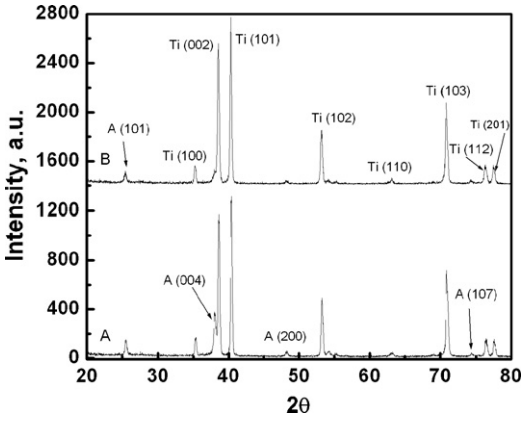

Fig. 5. X-ray diffraction patterns of (A) ethylene glycol ultrasonicated and N_2 annealed (EGUN) and (B) ethylene glycol ultrasonicated and H_2 annealed (EGUH) samples. A higher concentration of anatase phase of TiO_2 is observed in EGUN samples, especially evident by (0 0 4) reflection near $2\theta = 38^\circ$. "A (*h k l*)" indicates reflections due to anatase phase TiO_2.

3.4. Effect of varying bias voltage

Hitherto the degradation of MO has been studied at an arbitrary +0.6 V versus SCE. Generally, higher rates of degradation have been reported with increase in external bias [33,34]. To determine the minimum level of applied bias required to initiate improvement in degradation of MO, the bias was decreased from +0.6 to +0.0 V in steps of 0.1 V. The effects of this change in the external bias on MO degradation over EGUN are shown in Fig. 6. Remarkably, a near-complete degradation was observed around $t = 60$ min even at a low bias level of +0.1 V. Additionally, complete degradation was observed around $t = 45$ min for all bias voltages greater than or equal to +0.1 V.

One can notice that a substantial portion (~90%) of the dye is degraded within the first 20 min even at a low potential of +0.1 V. Further illumination only facilitates in the removal of the trace dye from the solution. It is also observed that any further increase in the applied bias beyond +0.3 V does very little to enhance the degradation rate.

3.5. Recyclability of TiO_2 NT catalyst

Rigorous analysis of the stability of the TiO_2 NTs was performed by examining their ability to facilitate degradation of fresh dye

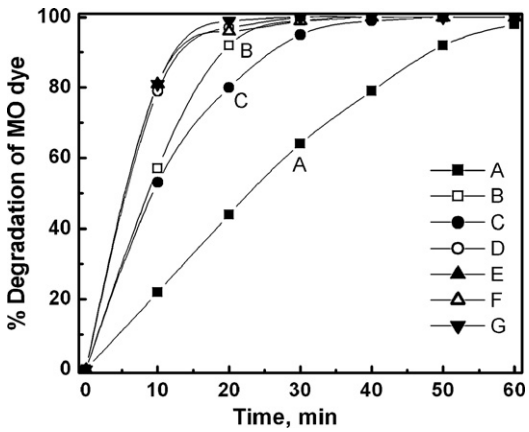

Fig. 6. Effect of increasing bias potential on degradation rate of MO dye under UV–vis illumination: (A) +0.0 V, (B) +0.1 V, (C) +0.2 V, (D) +0.3 V, (E) +0.4 V, (F) +0.5 V, (G) +0.6 V with ethylene glycol ultrasonicated and N_2 annealed (EGUN) samples.

solutions. Fresh batches of 40 μM MO was degraded over EGUN at +0.4 V as shown in Fig. 7. It was noted that in all instances the TiO_2 NTs completely degrades MO within 30 min. It is important to mention that the TiO_2 was not cleaned prior to its use between each batch of fresh MO solutions.

At times, in particulate films, dye degradation efficiency can reduce due to long term or multiple use of the TiO_2 film [35]. This can be attributed to the possible adsorption of intermediates over TiO_2 active sites which might render the catalyst site unusable for degradation of fresh dye molecules [36] (and references there in).

From Fig. 7, it can be noted that reproducible degradation without loss of activity is possible even with reuse (A: 1st cycle, B: 3rd cycle). The slight decrease in the initial rate (0 to 10 min) can be observed, only after a few cycles (C: 6th cycle). This decrease in activity can be recovered simply by ultrasonicating the TiO_2 nanotubes in distilled water for few minutes (Curve (D)).

Our data suggests that the degradation of the MO dye over TiO_2 nanotubes at +0.4 V does show significant change in the degradation ability of the TiO_2. In this work, we did not examine the nanotubes for any residual intermediates. However, the fact that the degradation rate is almost identical, suggests that even if there was an intermediate adsorbed on the surface, it is inconsequential and does not interfere with the degradation of a fresh batch of dye till the sixth cycle. Further analysis using spectroscopy to explore the TiO_2 surface after degradation can reveal the extent of adsorbed intermediates.

3.6. Effect of presence of oxidants

We measured and found that the external bias of +0.0 V is significant compared to Voc. We measured the rest potential under illumination to be −350 mV versus calomel electrode (anodically polarized). The purpose of performing the photocatalysis with no bias was to examine the extent of degradation in the absence of anodic polarization. We also examined the effects of addition of common oxidizing species on the MO degradation. This includes oxygen and hydrogen peroxide.

3.6.1. Addition of oxygen

Oxygen acts as a scavenger for the photogenerated electrons to form superoxide ions ($O_2 + e^- \rightarrow O_2^-$) and thus promotes charge separation. This allows the photogenerated holes and $OH^\bullet$, strong oxidizing species, to accelerate degradation rates. Therefore, the addition of molecular oxygen on the photoelectrocatalytic degradation of MO dye was examined at +0.0 V external bias and under no external bias conditions. The effect of saturating the MO solution with oxygen is shown in Fig. 8. It can be observed that absence of an external bias and absence of oxygen demonstrate very low MO degradation (~20%). However, when oxygen is added under no external bias, an improvement in the dye degradation rates from 20% to 50% is noted (Curves (A) and (B)). On the other hand, under an external bias of +0.0 V, only a marginal improvement in the dye degradation in the presence of oxygen is noted (Curves (C) and (D)).

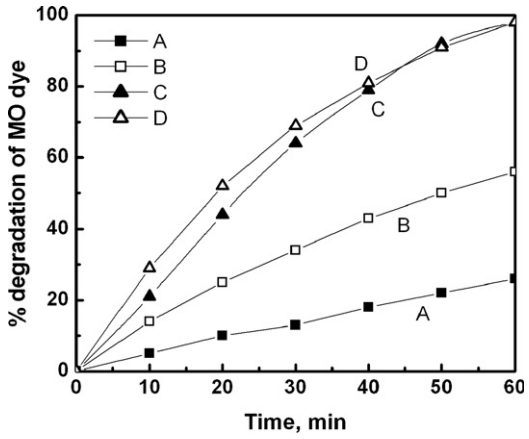

Fig. 8. Degradation under: (A) no bias, no oxygen addition, (B) no bias, with oxygen addition, (C) +0.0 V, no oxygen addition, and (D) +0.0 V, with oxygen addition. All experiments were performed under UV/vis illumination with ethylene glycol ultrasonicated and N_2 annealed (EGUN) samples.

3.6.2. Addition of hydrogen peroxide

It has been reported that the addition of hydrogen peroxide also increases the dye degradation efficiency of TiO_2 in slurry reactors [37]. This is because H_2O_2 produce strong oxidizing hydroxyl radical by dissociation ($H_2O_2 \leftrightarrow 2OH^\bullet$) that facilitate improve oxidation of the dyes [38]. To determine whether this holds true for nanotubular TiO_2, hydrogen peroxide was added (2.64 wt.%) to the MO solution. The degradation was carried out under +0.0 V external bias as well as under no external bias conditions.

It can be noted from Fig. 9 that the addition of H_2O_2 yields a higher rate of degradation regardless of the application of bias. Under no bias conditions, the addition of H_2O_2 can increase the

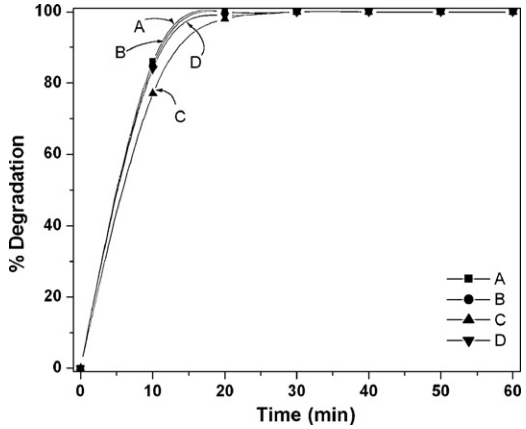

Fig. 7. Effect of reuse of catalyst: (A) 1st run, (B) 3rd run, (C) sixth run, and (D) 1st run after ultrasonication of the nanotubes in DI water for a few minutes. All experiments were performed at +0.4 V with UV–vis illumination on a single sample of ethylene glycol ultrasonicated and N_2 annealed (EGUN).

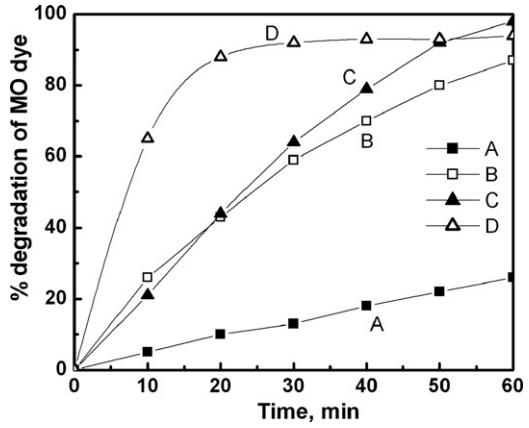

Fig. 9. Effect of addition of 2.64 wt.% hydrogen peroxide on the degradation: (A) no bias, without peroxide; (B) no bias, with peroxide; (C) +0.0 V, without peroxide; and (D) +0.0 V, with peroxide. All experiments were performed under UV/vis illumination with ethylene glycol ultrasonicated and N_2 annealed (EGUN) samples.

degradation from 20% to 85% over a 60 min period (Curves (A) and (B)). Further, with +0.0 V bias, a remarkable increase in the initial rate of degradation is observed (Curve (D)); by t = 20 min, nearly 90% of the dye is degraded. However, the degradation rate levels out around t = 30 min, and a minimal amount of further degradation is observed beyond this point. +0.0 V without the addition of hydrogen peroxide (Curve (C)) appears to be a better option for complete degradation of the dye molecules compared to Curve (D). At t = 50 min, Curve (C) catches up with Curve (D) ultimately leading up to a near-complete degradation (99%).

4. Discussion

Efficient charge separation, light absorption, and ability to scavenge photogenerated charges are some of the properties desired of a good photocatalyst [39,40]. Unlike nanoparticles, anodized TiO_2 nanotubes have a regular structure with less grain boundary than nanoparticles. This provides shorter charge diffusion path which helps in promoting charge transport in TiO_2 nanotubes [27]. Greater charge separation is essential for improving the redox properties (e.g., hole mediated photo-oxidation) at the catalyst surface. It is believed that this improved catalytic activity of the nanotube is due to the well-developed epitaxial structure of the TiO_2 tubes devoid of recombination centers, which are typical in a particulate film. This property of TiO_2 nanotubes has been exploited for several solar-based application such as water splitting to produce hydrogen and electricity generation (photovoltaics) [41].

The results discussed so far shows that TiO_2 nanotubes prepared in ethylene glycol under ultrasonication (EGU) can demonstrate some of the above properties and hence can be considered as a likely candidate for the degradation of textile effluents. Among the different methods examined in this study, the ultrasound method facilitates the formation of much longer TiO_2 nanotubes within shorter duration of time compared to the stirring method. It is reported that ultrasound facilitates mass transport resistance-free movement of the electrolyte species to the metal–oxide interface which enables in the development of uniform nanotubes [28]. Greater light absorbance by the longer nanotubes can be one reason for better performance of the EGUN, EGUH nanotubes compared to the stirred samples.

Further, on comparing the EG with PA, EG has been noted to introduce carbon into the structure of the TiO_2 nanotubes [28]. Employing EG as an electrolyte for synthesis of the nanotubes has been noted to improve the photoelectrochemical properties of the TiO_2. It is therefore possible that the doping of carbon into the TiO_2 structure can facilitate in the improvement of visible light absorbance. This can boost the catalytic performance of the EG based TiO_2 (note that we have employed UV–vis light in this work for photo-illumination). To verify possible contribution from carbon doping, the effect of visible light on the dye degradation is currently being investigated.

We also examined the pathway for MO degradation. Oxidation of dyes such as MO can occur by the hydroxyl radical and/or holes formed during the photo-illumination at the semiconductor surface. The hydroxyl radicals are particularly strong oxidizing species formed over TiO_2 from adsorbed water and/or hydroxyl ions [42]. Different methods of dye oxidation by hydroxyl radicals and holes are discussed in a recent article [43]. Further, of relevance to this work is an interesting result reported by Xie and coworkers where they discuss the formation of *in situ* H_2O_2 over TiO_2 nanotube during photo-illumination [24]. The proposed mechanism suggests that O_2 can scavenge the electrons from the photocathode and react in the presence of H^+ ions to produce H_2O_2. O_2 is also well known to scavenge electrons from the photoanode immediately following illumination [11,44]. The application of external bias assists in decreasing loss of electrons due to recombination with holes as well as reacting with oxygen. From these observations it is reasonable to expect that the electrons could either be scavenged at the anode or pass through the external circuit and then react with the different surrounding species in the electrolyte at the cathode surface.

To better understand the reaction processes one can monitor the change in the photocurrent during the continuous illumination of the cell. Since we noticed an improvement in dye degradation even at low potential, we choose to monitor the photocurrent during the dye degradation under an external bias of +0.0 V in the presence of oxygen. Our goal was to follow the changes in the photocurrent (if any) during the prolonged illumination of the cell and examine if the changes in the electrolyte saturation conditions has any effect on the photocurrent. Fig. 10 shows the photocurrent monitored in the presence of oxygen and nitrogen. The photocurrent was noted to increase initially and then stabilize in about 40 min during illumination at +0.0 V in the presence of nitrogen. In the presence of oxygen, however, the photocurrent is noted to decrease with time.

In the nitrogen gas saturated solution, most of the photogenerated electrons move through the external circuit which is indicated by the rising current. At the cathode the electrons can

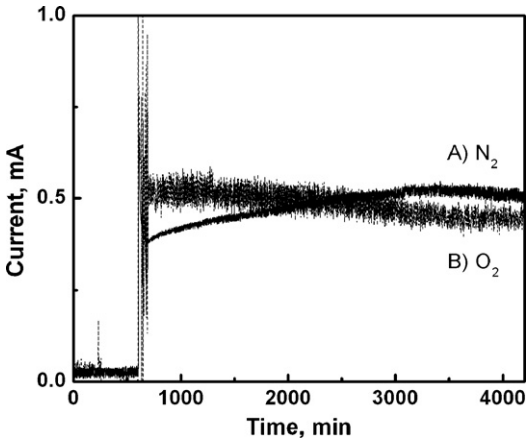

Fig. 10. Photocurrent profile generated during degradation under (A) nitrogen saturation and (B) oxygen saturation. All experiments were performed under UV/vis illumination at +0.0 V with ethylene glycol ultrasonicated and N_2 annealed (EGUN) samples.

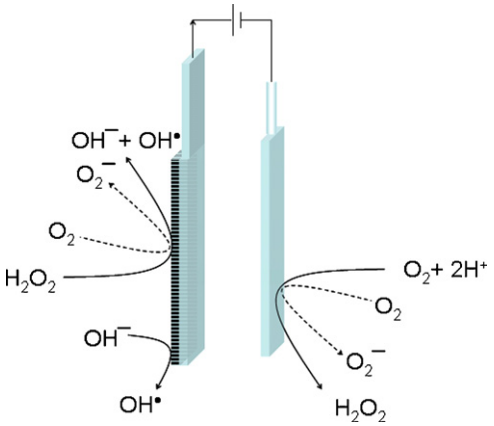

Scheme 1. Pathway for electron scavenging at the anode and cathode during illumination of the TiO_2 nanotubes in oxygen and nitrogen saturated solution.

react with oxygen and H^+ ions as proposed by Xie and coworkers to form H_2O_2 [24,45]. With continuous illumination, the H_2O_2 concentration begins to increase, and it starts to compete for electrons formed at the anode to form hydroxyl radicals (refer to Scheme 1). This can cause a decrease in the photocurrent as noted in Fig. 10. On the other hand, when the solution is saturated with oxygen it begins to scavenge electrons from anode immediately following photo-illumination. As the illumination continues, H_2O_2 formed at the cathode accelerates the scavenging of electrons from the anode. These cumulative effects contribute to the steady decline in the photocurrent noted in Fig. 10 in the presence of oxygen.

5. Conclusion

The degradation of a model textile dye methyl orange over TiO_2 nanotubes prepared by anodization in different electrolytes has been presented. It is shown that TiO_2 nanotubes prepared under ultrasonication demonstrate better degradation of the dye than those prepared by stirring the anodizing medium. Nanotubes prepared in ethylene glycol demonstrate a substantial improvement in degradation compared to those prepared in phosphoric acid. Application of as low as +0.1 V external bias dramatically improves the degradation of the dye. Addition of oxidizing agents such as oxygen and H_2O_2 promotes the degradation of the dye. By monitoring the photocurrent, it is possible to predict the photocatalytic reactions at the TiO_2 nanotube surface.

Acknowledgements

VS would like to thank Dr. Misra for providing laboratory support used for the characterization of the TiO_2 nanotubes. Support of the Mackay School of Earth Sciences and Engineering research facilities for X-ray analysis is also appreciated. The financial support of the Department of Energy (Grant # DE-FC 3606GO86066) is also acknowledged.

References

[1] H. Zollinger, Color Chemistry: Syntheses, Properties and Applications of Organic Dyes and Pigments, 2nd ed., VCH, New York, 1991.
[2] U. Pagga, K. Taeger, Water Res. 28 (1994) 1051–1057.
[3] M.A. Zanjanchi, A. Ebrahimian, Z. Alimohammadi, Opt. Mater. 29 (2007) 794–800.
[4] G.K. Parshettia, S.D. Kalmea, S.S. Gomarea, S.P. Govindwar, Bioresource Technol. 98 (2007) 3638–3642.
[5] S.B. Xia, S.C. Xia, C.Q. Zhu, J. Hazard. Mater. 144 (2007) 159–163.
[6] Y.G. Adewuyi, Environ. Sci. Technol. 39 (2005) 8557–8570.
[7] D. Bahnemann, Sol. Energy 77 (2004) 445–459.
[8] H. Gerischer, Electrochim. Acta 40 (1995) 1277–1281.
[9] H. Lachheb, E. Puzenat, A. Houas, M. Ksibi, E. Elaloui, C. Guillard, J.M. Herrmann, Appl. Catal. B: Environ. 39 (2002) 75–90.
[10] M. Vautier, C. Guillard, J.M. Herrmann, J. Catal. 201 (2001) 46–59.
[11] M.F.J. Dijkstra, A. Michorius, H. Buwalda, H.J. Panneman, J.G.M. Winkelman, A.A.C.M. Beenackers, Catal. Today 66 (2001) 487–494.
[12] H. Sayilkan, Appl. Catal. A: Gen. 319 (2007) 230–236.
[13] V. Subramanian, P.V. Kamat, E.E. Wolf, Ind. Eng. Chem. Res. 42 (2003) 2131–2138.
[14] M.E. Osugi, G.A. Umbuzeiro, F.J.V. De Castro, M.V.B. Zanoni, J. Hazard. Mater. 137 (2006) 871–877.
[15] M.V.B. Zanoni, J.J. Sene, M.A. Anderson, J. Photochem. Photobiol. A 157 (2003) 55–63.
[16] P.A. Carneiro, M.E. Osugi, J.J. Sene, M.A. Anderson, M.V.B. Zanoni, Electrochim. Acta 49 (2004) 3807–3820.
[17] M.E. Osugi, G.A. Umbuzeiro, M.A. Anderson, M.V.B. Zanoni, Electrochim. Acta 50 (2005) 5261–5269.
[18] M. Noorjahan, M.P. Reddy, V.D. Kumari, B. Lavedrine, P. Boule, M. Subrahmanyam, J. Photochem. Photobiol. A 156 (2003) 179–187.
[19] D. Gong, C.A. Grimes, O.K. Varghese, W.C. Hu, R.S. Singh, Z. Chen, E.C. Dickey, J. Mater. Res. 16 (2001) 3331–3334.
[20] J.M. Macak, H. Tsuchiya, P. Schmuki, Angew. Chem.-Int. Ed. 44 (2005) 2100–2102.
[21] K.S. Raja, T. Gandhi, M. Misra, Electrochem. Commun. 9 (2007) 1069–1076.
[22] K.S. Raja, M. Misra, V.K. Mahajan, T. Gandhi, P. Pillai, S.K. Mohapatra, J. Power Sources 161 (2006) 1450–1457.
[23] J.M. Macak, M. Zlamal, J. Krysa, P. Schmuki, Small 3 (2007) 300–304.
[24] Y. Xie, Electrochim. Acta 51 (2006) 3399–3406.
[25] S.G. Yang, Y.Z. Liu, C. Sun, Appl. Catal. A: Gen. 301 (2006) 284–291.
[26] M. Zlamal, J.M. Macak, P. Schmuki, J. Krysa, Electrochem. Commun. 9 (2007) 2822–2826.
[27] R. Beranek, H. Tsuchiya, T. Sugishima, J.M. Macak, L. Taveira, S. Fujimoto, H. Kisch, P. Schmuki, Appl. Phys. Lett. 87 (2005), 243114, 243111–243113.
[28] S.K. Mohapatra, M. Misra, V.K. Mahajan, K.S. Raja, J. Catal. 246 (2007) 362–369.
[29] S. Al-Quadawi, S.R. Salman, J. Photochem. Photobiol. A 148 (2002) 161–168.
[30] S.D. Sharma, D. Singh, K.K. Saini, C. Kant, V. Sharma, S.C. Jain, C.P. Sharma, Appl. Catal. A: Gen. 314 (2006) 40–46.
[31] Z. Liu, X. Zhang, S. Nishimoto, M. Jin, D. Tryk, T. Murakami, A. Fujishima, J. Phys. Chem. C 112 (2008) 253–259.
[32] M. Tian, G. Wu, B. Adams, J. Wen, A. Chen, J. Phys. Chem. C 112 (2008) 825–831.
[33] R.J. Candal, W.A. Zeltner, M.A. Anderson, Environ. Sci. Technol. 34 (2000) 3443–3451.
[34] Z.H. Zhang, Y. Yuan, G.Y. Shi, Y.J. Fang, L.H. Liang, H.C. Ding, L.T. Jin, Environ. Sci. Technol. 41 (2007) 6259–6263.
[35] K.V.S. Rao, M. Subrahmanyam, P. Boule, Appl. Catal. B: Environ. 49 (2004) 239–249.
[36] C.G. Silva, W.D. Wang, J.L. Faria, J. Photochem. Photobiol. A 181 (2006) 314–324.
[37] C. Hachem, F. Bocquillon, O. Zahraa, M. Bouchy, Dyes Pigments 49 (2001) 117–125.
[38] M. Huang, C. Xu, Z. Wu, Y. Huang, J. Lin, J. Wu, Dyes Pigments 77 (2008) 327–334.
[39] G.K. Mor, O.K. Varghese, M. Paulose, K. Shankar, C.A. Grimes, Sol. Energy Mater. Sol. Cells 90 (2006) 2011–2075.
[40] K.S. Raja, V.K. Mahajan, M. Misra, J. Power Sources 159 (2006) 1258–1265.
[41] G.K. Mor, K. Shankar, M. Paulose, O.K. Varghese, C.A. Grimes, Appl. Phys. Lett. 91 (2007) 152111.
[42] C.S. Turchi, D.F. Ollis, J. Catal. 122 (1990) 178–192.
[43] G. Sivalingam, K. Nagaveni, M.S. Hegde, G. Madras, Appl. Catal. B: Environ. 45 (2003) 23–38.
[44] N. Serpone, I. Texier, A.V. Emeline, P. Pichat, H. Hidaka, J. Zhao, J. Photochem. Photobiol. A 136 (2000) 145–155.
[45] Y. Xie, L. Zhou, H. Huang, Appl. Catal. B: Environ. 76 (2007) 15–23.